

Nickel precipitation at nanocavities in separation by implantation of oxygen

Miao Zhang

Department of Physics and Material Sciences, City University of Hong Kong, 83 Tat Chee Avenue, Kowloon, Hong Kong and State Key Laboratory of Functional Materials for Informatics, Shanghai Institute of Metallurgy, Chinese Academy of Sciences, Shanghai 200050, China

Xuchu Zeng and Paul K. Chu^{a)}

Department of Physics and Material Sciences, City University of Hong Kong, 83 Tat Chee Avenue, Kowloon, Hong Kong

R. Scholz

Max-Planck-Institute of Microstructure Physics, Weinberg 2, D-06120, Halle, Germany

Chenglu Lin

State Key Laboratory of Functional Materials for Informatics, Shanghai Institute of Metallurgy, Chinese Academy of Sciences, Shanghai 200050, China

(Received 9 September 1999; accepted 2 June 2000)

The structures of nickel decorated cavities and Ni precipitates epitaxially grown in the nanocavity band in separation by implantation of oxygen (SIMOX) are studied. The nanocavities are generated in the silicon substrate of the SIMOX wafer by proton implantation followed by Ni implantation into the Si overlayer. Channeling Rutherford backscattering spectrometry results indicate that Ni implantation changes the crystalline Si overlayer into amorphous Si. After annealing at 1000 °C for 2 h, the amorphous Si evolves into a polycrystalline structure composed of NiSi₂ and polycrystalline silicon. In the meantime, most of the nickel atoms diffuse through the buried oxide layer and are gettered by the nanocavity band. NiSi₂ precipitates are observed both in the nanocavities and at the residual defects created by H implantation. The microstructure of the Ni precipitate depends on whether there are cavities nearby. Without cavities in the vicinity, dislocations are observed in the neighborhood of the precipitate, whereas no dislocation is detected around the precipitate when there are nanocavities in the neighborhood. The precipitation and gettering behavior can be explained by the gettering of Si interstitials to the microcavities and lowering of the nucleation barrier. © 2000 American Vacuum Society. [S0734-2101(00)06605-7]

I. INTRODUCTION

Transition metals are common impurities in silicon originating from the crystal growth and subsequently integrated circuits (IC) fabrication steps. They are typically detrimental to the ICs because they can degrade the minority carrier lifetime and increase the junction leakage current.¹ The increasing complexity and miniaturization of modern integrated circuits require higher yield and hence a smaller density of defects and impurities in the electrically active zone of devices. Various kinds of gettering methods such as P diffusion,² internal gettering (IG),³ and carbon implantation⁴ have been developed to remove the impurities to a sacrificial region. Recently, a technique using microcavities created by H or He ion implantation has been extensively studied and shown to be effective in trapping Cu, Ni, Au, and Pt in bulk Si.^{5–10}

For high speed, low power, complementary metal–oxide–semiconductor (CMOS) devices, silicon-on-insulator (SOI) has many advantages over bulk Si.¹¹ Separation-by-implantation-of-oxygen (SIMOX) is the most widely used commercial SOI material. The manufacturing process utilizes high dose oxygen implantation into silicon at elevated

temperature followed by annealing at above 1300 °C. Transition metal impurities may contaminate the SIMOX wafers during oxygen implantation, high temperature annealing, and other handling processes. Nanocavities generated by He or H implantation have been proposed to getter Cu and Fe in SIMOX.^{12–15} The results suggest that these nanocavities are more effective for Cu than for Fe. Nickel is a common impurity in IC processes, and its high diffusivity and reactivity make it highly deleterious, but the mechanism of Ni gettering to nanocavities in SIMOX has not been demonstrated. Mohadjeri *et al.*⁷ studied gettering of high dose implanted Ni ($1 \times 10^{15} \text{ cm}^{-2}$) to the H-implantation-induced nanocavities in bulk Si and found that the amorphous silicon (α -Si) caused by Ni implantation reduced the gettering efficiency. In this study, we investigate the mechanism of nanocavity gettering of Ni in SIMOX. Our results demonstrate that although the polycrystalline Si (poly-Si) formed in the overlying silicon layer can getter Ni by annealing, 38% of the implanted Ni diffuses through the buried oxide (BOX) and saturates the dangling bonds on the cavity walls or form precipitates in the cavity band. The dislocation microstructure caused by the Ni precipitates depends on whether there are nanocavities in the vicinity.

^{a)}Electronic mail: paul.chu@cityu.edu.hk

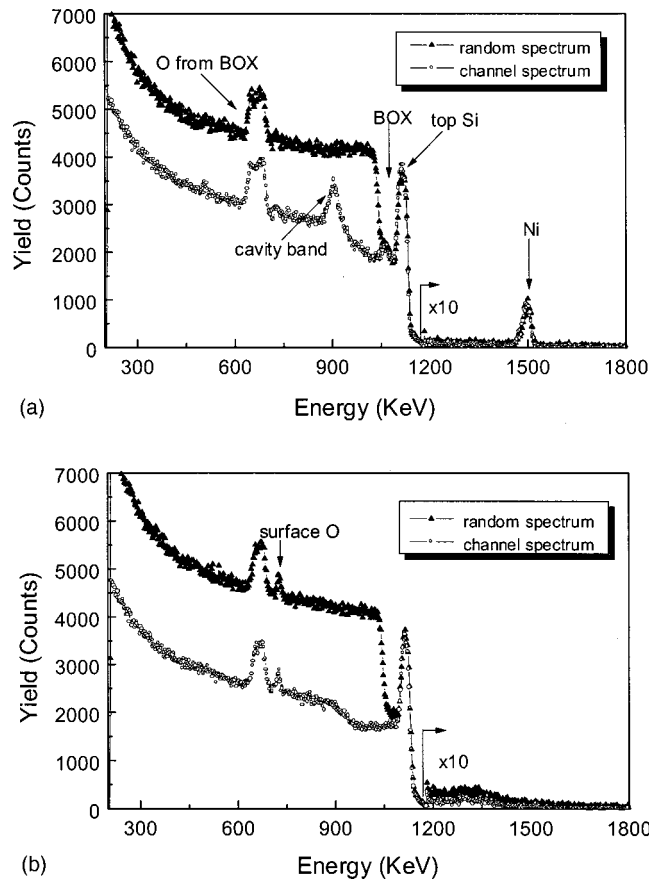


Fig. 1. RBS/channeling spectra of the $3.5 \times 10^{16} \text{ cm}^{-2} \text{ H}^+$ and $2 \times 10^{15} \text{ cm}^{-2} \text{ Ni}^+$ implanted SIMOX: (a) Before annealing. (b) After annealing at 1000°C for 2 h.

II. EXPERIMENT

The SIMOX wafer was produced in our laboratory by implanting $5 \times 10^{17} \text{ atoms/cm}^{-2} \text{ O}^+$ into an *n*-type (100) Si at 70 keV and a substrate temperature of 680°C , followed by annealing at 1300°C for 6 h in Ar+0.5% O_2 . The SIMOX wafer was implanted with 50 keV, $3.5 \times 10^{16} \text{ cm}^{-2} \text{ H}^+$ at room temperature followed by annealing at 700°C for 30 min to form a band of cavities beneath the buried oxide (BOX) layer. A dose of $2 \times 10^{15} \text{ cm}^{-2} \text{ Ni}$ was implanted into the top Si layer at 70 keV at room temperature. The specimen was then annealed at 1000°C for 2 h in a nitrogen atmosphere to redistribute the Ni impurities. The depth profiles of Ni and damage caused by Ni and H implantation before and after 1000°C annealing were investigated by 2 MeV He channeling Rutherford backscattering spectrometry (RBS/C). The scattering angle was set at 170° . The microstructure of the sample after 1000°C annealing was examined by cross-sectional transmission electron microscopy (XTEM) using a 200 kV Philips CM-20T or 400kV Philips JEM-400EX.

III. RESULTS AND DISCUSSION

RBS/C was carried out to characterize the H and Ni implanted SIMOX before and after annealing at 1000°C , and

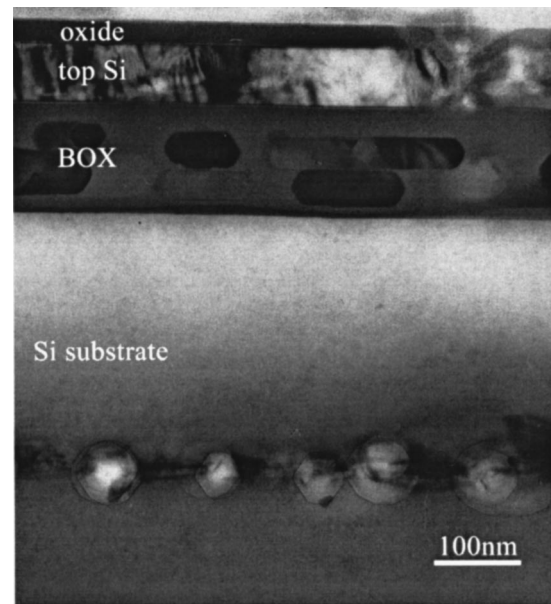


Fig. 2. XTEM bright-field image of the SIMOX sample implanted with $3.5 \times 10^{16} \text{ cm}^{-2} \text{ H}^+$ and $2 \times 10^{15} \text{ cm}^{-2} \text{ Ni}^+$, followed by annealing at 1000°C for 2 h. A narrow cavity band has formed beneath the buried oxide layer. The micrograph was acquired at 200 kV using a Philips CM-20T.

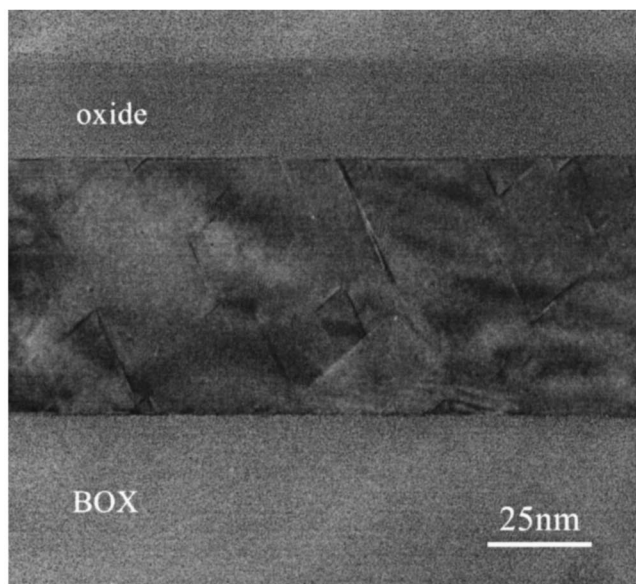
the results are exhibited in Fig. 1. Figure 1(a) depicts the spectrum acquired from the as-implanted sample. Three regions, top Si, buried oxide (BOX), and Si substrate, can be observed. Comparing the random and the aligned spectra, the backscattering yield in the channeling spectrum of the top Si is similar to that of the random spectrum demonstrating that the top Si layer has been transformed into an amorphous layer by Ni implantation. The peak of the Ni depth profile is at the middle of the Si overlayer. The H implantation induced damage zone can also be observed. Figure 1(b) shows the RBS/C results of the annealed sample. After 1000°C annealing, no Ni peak is detected by RBS, suggesting that Ni has moved into the wafer after this thermal treatment and the Ni concentration left in the top Si has diminished to below the detection limit of RBS. The damage peak introduced by H implantation has decreased greatly. Furthermore, in addition to the oxygen signal from the BOX, another oxygen signal originating from the sample surface is seen indicating that the sample surface has been oxidized during thermal treatment. It is expected that the α -Si caused by Ni implantation will undergo recrystallization at such a high annealing temperature. However, as shown in Fig. 1(b), the backscattering yield in the channeling spectrum corresponding to the top Si layer is still equal to that of the random spectrum. This shows that the top Si has not become single crystal after 1000°C annealing. Further XTEM study reveals that the top Si has a polycrystalline structure consisting of Ni precipitates and polycrystalline silicon.

Figure 2 is the XTEM image of the SIMOX sample implanted with $3.5 \times 10^{16} \text{ cm}^{-2} \text{ H}$ and $2 \times 10^{15} \text{ cm}^{-2} \text{ Ni}$ after annealing at 1000°C for 2 h. The thickness of the top Si and BOX is 65 and 120 nm, respectively. About 25 nm of surface Si has been oxidized during annealing, which is in agreement

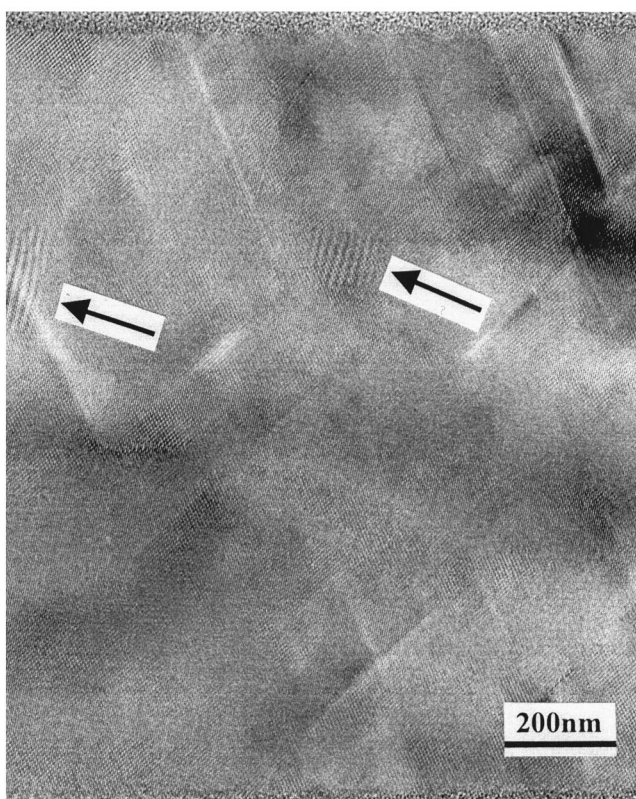
with the RBS result in Fig. 1(b). The original silicon overlayer is thick enough (about 90 nm thick) to stop the implanted nickel ions, which were calculated to have a projected range of 50 nm using TRIM94. The BOX contains typical Si islands, and a nanocavity band has formed about 300 nm below the BOX layer. The diameter of the nanocavities varies from 10 to 130 nm (although not shown here, voids as large as 130 nm were observed in this study), and some of the nanocavities have evolved into a faceted shape to decrease the surface energy. No defects such as stacking faults stemming from the SIMOX production process are detected in the region just below the BOX layer.

Figure 3(a) shows the XTEM micrograph of the top Si layer after 1000 °C annealing and Fig. 3(b) is a magnified image of Fig. 3(a). It is evident that the top Si has been transformed into a polycrystalline structure. Since the lattice mismatch between NiSi₂ and crystalline silicon is very small (only 0.4% at room temperature),¹⁶ it is difficult to distinguish the Ni precipitates from poly-Si. However, the Moiré fringes characteristic of a second bulk phase can be observed in the top Si layer near the projected range of Ni. This demonstrates that NiSi₂ precipitates have formed in the top Si layer after annealing.

Figures 4–6 depict the structure of the nanocavity band in the H and Ni implanted SIMOX after annealing. Figure 4 is a dark field XTEM picture whereas Figs. 5 and 6 are bright field XTEM images. It has been proposed that metallic impurities diffusing to a cavity band will first be captured by the dangling bonds on the walls.⁶ Subsequently, the impurities may precipitate in the cavities after the dangling bonds on the walls are occupied (saturated).⁷ XTEM cannot detect atomic Ni trapped on the void walls, but bulk phase Ni precipitates can be observed. In this study, precipitate-filled cavities are observed. Most of the cavities in Fig. 4 exhibit a dark appearance and one cavity has a white appearance. The white cavity in this dark field image is filled with Ni bulk phase precipitate. Figure 5 shows the morphology of three nanocavities. The nanocavities on the left and in the middle of the picture have a darker appearance than the surrounding Si matrix, indicating Ni precipitation in the nanocavities after the dangling bonds on the cavity walls are saturated with Ni. In a previous study,¹⁵ we studied Cu gettering to cavities produced by H and He implantation in SIMOX and only observed Cu precipitate-filled cavities in the H-implanted sample which contains less nanocavities (thus less dangling bonds) than the He-implanted SIMOX sample. Ni precipitate-filled cavities have been observed,⁷ but Ni precipitation at the defects in the cavity band has not been reported. Our data reveal that Ni precipitates can form in other locations in the cavity band. {111} faceted Ni precipitates are observed in the neighborhood of nanocavities as shown in Figs. 6(a) and 6(b), and this observation is in line with the previous report that nickel precipitates in the form of crystalline silicides epitaxially grown on defined planes of the silicon host lattice.^{17,18} In Fig. 6(a), there is only one small cavity near the big precipitate, and dense dislocations are observed near the precipitate. Some of the big dislocations



(a)



(b)

Fig. 3. (a) XTEM bright-field micrograph of the top silicon layer after 1000 °C annealing. (b) A magnified image of (a). Grain boundaries and Moiré fringes can be observed. The micrographs were taken at 400 kV using a Philips JEM-400EX.

extend from the H implantation damage peak to the lower edge of the BOX. These dislocations apparently propagate from the precipitate during formation. When such a precipitate is present near nanocavities [Fig. 6(b)], no dislocation is

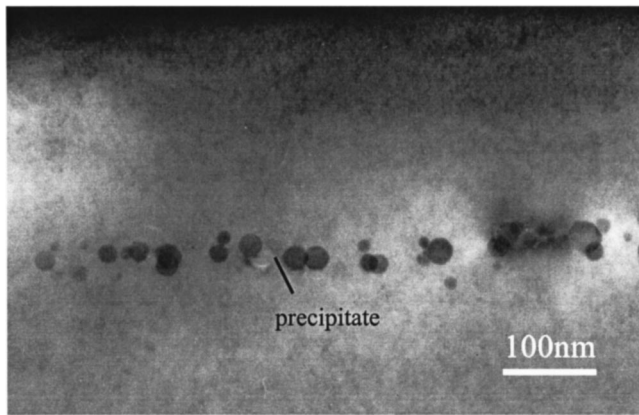


FIG. 4. XTEM dark-field picture of the nanocavities. A nanocavity filled with Ni precipitate is indicated. The micrograph was taken at 400 kV using a Philips JEM-400EX.

formed around it, but strain fields can be observed around the nanocavities.

In this study, epitaxially grown NiSi_2 is observed in both the top Si overlayer and microcavity band after annealing, but the NiSi_2 growth mechanisms in the two locations are quite different. Ni silicide forms in the α -Si in the top layer, whereas Ni precipitates epitaxially along the crystalline silicon in the cavity band. Before annealing, all the implanted Ni impurities are in the α -Si. Upon 1000 °C annealing, the α -Si in the top layer recrystallizes. Meanwhile, Ni precipitates form at the concentration peak of Ni. The formation of silicide has been shown to facilitate the recrystallization of α -Si.¹⁹ Some Ni impurities diffuse through the BOX layer into the substrate. Although poly-Si can trap Ni impurity effectively,²⁰ quantitative secondary ion mass spectroscopy (SIMS) measurements (not shown here) show that 38% of the implanted Ni (corresponding to a dose of $7.6 \times 10^{14} \text{ cm}^{-2}$) has been captured in the nanocavity band. We have found that nickel precipitates epitaxially at the cavity band (Fig. 6). The formation mechanism of precipitates in the cavity band can be categorized as relaxation gettering²¹ and is based on the heterogeneous precipitation of impurities at nuclei formed by lattice defects.

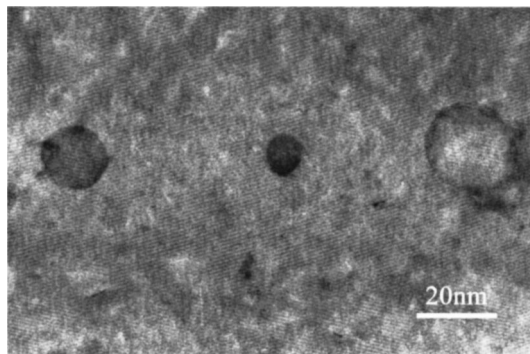
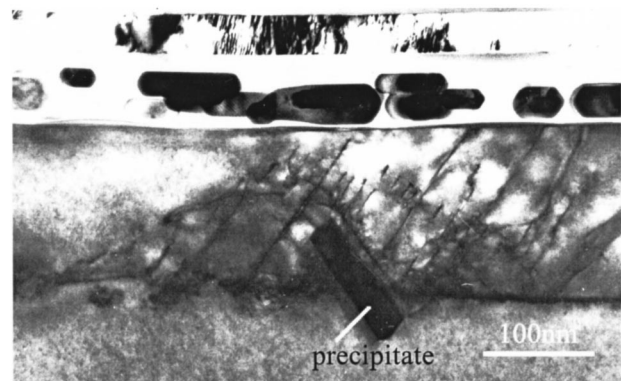
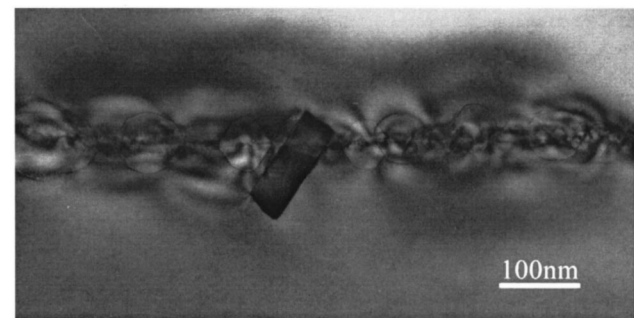


FIG. 5. XTEM bright-field image of the H and Ni implanted SIMOX after 1000 °C annealing showing three nanocavities with different contrast. The micrograph was taken at 400 kV using a Philips JEM-400EX.



(a)



(b)

FIG. 6. XTEM bright-field image of the H, Ni implanted SIMOX after 1000 °C annealing revealing precipitates in the H-implantation band: (a) A Ni precipitate with dislocations. The dark string at the H projected range cutting through the Ni precipitate is probably decorated with nickel. (b) A Ni precipitate with many nanocavities near it. No dislocations are detected around this precipitate. The micrographs were taken at 400 kV using a Philips JEM-400EX.

After 1000 °C annealing, Ni precipitates with [Fig. 6(a)] and without [Fig. 6(b)] dislocations are formed in the residual defects in the cavity band. The difference in the precipitates can be attributed to the adsorption of Si interstitials to the nanocavities. The lattice parameter of NiSi_2 is larger than that of silicon at temperature above 500 °C.²² Therefore, silicon self-interstitials are emitted leading to the formation of extrinsic dislocations in the surrounding silicon matrix as exhibited in Fig. 6(a). NiSi_2 epitaxially grown on c -Si with dislocations in a Si matrix has been reported.^{18,23} However, things are different when there are nanocavities in the vicinity of the Ni precipitate. The absence of dislocation displayed in Fig. 6(b) is due to the gettering of point defects to the nanocavities. The nickel precipitation mechanism in nanocavities is similar to that of the surface silicide proposed by Seibt *et al.*, who suggested that impurities tend to precipitate at the sample surface due to a lowering of the nucleation barrier.²² It is expected that the sample surface acts as a sink for silicon self-interstitials and vacancies generated during precipitation. The adsorption of interstitials to the microcavities has been reported by Raineri and Campisano.²⁴ The presence of cavities thus facilitates the growth of nickel precipitates at the residual defects in the H implantation induced damage region.

IV. CONCLUSION

Nanocavities are produced in the substrate of a SIMOX wafer by hydrogen implantation and a high dose of Ni is implanted to change the c -Si overlayer into α -Si. XTEM measurements are used to investigate the competitive gettering of Ni to the nanocavity band and to the polycrystalline Si overlayer as well as the microstructure of the Ni-decorated cavities. Our results demonstrate that upon 1000 °C annealing, the α -Si induced by Ni implantation recrystallizes accompanied by some Ni precipitation in the top Si layer. However, 38% of the implanted Ni diffuses through the buried oxide layer and is captured in the nanocavity band in the silicon substrate. NiSi₂ precipitates observed in the nanocavities are epitaxially grown at the residual defects created by H implantation. The nanocavities act as the gettering sites for Si interstitials released during the formation of NiSi₂ precipitates, thereby facilitating the growth of NiSi₂ precipitates in the cavity band.

ACKNOWLEDGMENTS

The authors would like to thank E. Z. Luo and Dr. B. Sundaravel of the Chinese University of Hong Kong for the RBS/C measurements. The work was supported by Hong Kong Research Grants Council Earmarked Grant Nos. 9040344 and 9040412, City University of Hong Kong Strategic Research Grant Nos. 7000964 and 7001028, Chinese National Natural Science Foundation Grant No. 69906005, and Shanghai Youth Foundation under Grant No. 98QE14028.

¹K. Graff, in *Metal Impurities in Silicon-Device Fabrication* (Springer, New York, 1995).

- ²J. S. Kong and D. K. Schroder, *J. Appl. Phys.* **65**, 2974 (1989).
³R. A. Craven and H. W. Korb, *Solid State Technol.* **24**, 55 (1981).
⁴H. Wong, N. W. Cheung, and P. K. Chu, *Appl. Phys. Lett.* **52**, 889 (1988).
⁵S. M. Myers, D. M. Follstaedt, and D. M. Bishop, *Mater. Res. Soc. Symp. Proc.* **316**, 33 (1994).
⁶D. M. Follstaedt, S. M. Myers, G. A. Petersen, and J. W. Medernach, *J. Electron. Mater.* **25**, 151 (1996).
⁷B. Mohadjeri, J. S. Williams, and J. Wong-Leung, *Appl. Phys. Lett.* **66**, 1889 (1995).
⁸J. Wong-Leung, C. E. Ascheron, M. Petravic, R. G. Elliman, and J. S. Williams, *Appl. Phys. Lett.* **66**, 1231 (1995).
⁹J. Min, P. K. Chu, X. Lu, S. S. K. Iyer, and N. W. Cheung, *Thin Solid Films* **300**, 64 (1997).
¹⁰P. K. Chu and N. W. Cheung, *Mater. Chem. Phys.* **57**, 1 (1998).
¹¹J. P. Colinge, *Silicon-on-Insulator Technology, Materials to VLSI* (Kluwer, Boston, 1991).
¹²W. Skorupa, N. Hatzopoulos, R. A. Yankov, and A. B. Danilin, *Appl. Phys. Lett.* **67**, 2992 (1995).
¹³R. A. Yankov, N. Hatzopoulos, W. Skorupa, and A. B. Danilin, *Nucl. Instrum. Methods Phys. Res. B* **120**, 60 (1996).
¹⁴M. Zhang, C. L. Lin, P. L. Hemment, K. Gutjhr, and U. Gosele, *Appl. Phys. Lett.* **72**, 830 (1999).
¹⁵M. Zhang, C. L. Lin, X. Z. Duo, X. X. Lin, and Z. Y. Zhou, *J. Appl. Phys.* **85**, 94 (1999).
¹⁶M. Seibt and W. Schroter, *Philos. Mag. A* **59**, 337 (1989).
¹⁷P. K. Sinha and W. S. Glaunsinger, *J. Mater. Res.* **5**, 1013 (1990).
¹⁸M. Seibt and K. Graff, *J. Appl. Phys.* **63**, 4444 (1988).
¹⁹R. C. Cammarata, C. V. Thompson, C. Hayzelden, and K. N. Tu, *J. Mater. Res.* **5**, 2133 (1990).
²⁰S. Okuuchi, M. B. Shabani, T. Yoshimi, and A. Abe, *The Electrochemical Society Meeting, Montreal, 1997* (unpublished), Vol. 97-1, p. 566.
²¹D. Gilles and H. Ewe, in *Semiconductor Silicon*, edited by H. R. Huff, W. Bergholz, and K. Sumino (The Electrochemical Society, Pennington, NJ, 1994), Vol. 94-10, p. 772.
²²M. Seibt, W. Schroter, *Lokalisierung und Identifizierung von Mikrodefekten. Forschungsbericht, Bundesministerium für Forschung und Technologie FRG* (1989).
²³P. D. Augustus, *Semicond. Int.* **11**, 88 (1985).
²⁴V. Raineri and S. U. Campisano, *Appl. Phys. Lett.* **69**, 1783 (1996).